Inorg. Chem. **2008**, *47*, 3140−3143

Fabrication of Hierarchical ZnO Architectures and Their Superhydrophobic Surfaces with Strong Adhesive Force

Yanbo Li,[†] Maojun Zheng,[*,†] Li Ma,[‡] Miao Zhong,[†] and Wenzhong Shen[†]

Laboratory of Condensed Matter Spectroscopy and Opto-Electronic Physics, Department of Physics, and School of Chemistry & Chemical Technology, Shanghai Jiao Tong University, Shanghai 200240, People's Republic of China

Received November 2, 2007

Grid-structured ZnO microsphere arrays assembled by uniform ZnO nanorods were fabricated by noncatalytic chemical vapor deposition, taking advantage of morphologies of alumina nanowire pyramid substrates and ZnO oriented growth habits. Every ZnO microsphere (similar to the micropapilla on a lotus leaf surface) is assembled by over 200 various oriented ZnO nanorods (similar to the hairlike nanostructures on mircopapilla of a lotus leaf). This lotus-leaf-like ZnO micro-nanostructure films reveal superhydrophobicity and ultrastrong adhesive force to liquid. The realization of this hierarchical ZnO nanostructure film could be important for further understanding wettability of biological surfaces with micro-nanostructure and application in microfluidic devices.

1. Introduction

The assemblies of low-dimensional building blocks (nanodots, nanowires, nanobelts, and nanotubes, etc.) into hierarchical architectures on various substrates have attracted great interest because of the demands for many practical applications in functional devices.[1–3] As one of the most important oxide semiconductor materials, ZnO has attracted considerable attention due to its good optical, electrical, and piezoelectrical properties and its potential applications in diverse areas.[4] Various quasi-one-dimensional nanostructures of ZnO have been grown, including nanobelts,[5] nanowires,[6] nanotubes,[7] etc. Meanwhile, various self-organized hierarchical ZnO nanostructures, such as nanorings,[8] nanopropellers,[9] nanobridges,[10] nanonails,[10] and nanocombs,[11–13] have been synthesized by vapor-phase processes. The novel functions of these ZnO nanostructures arrays have been revealed successfully in the nanolasings,[14] piezoelectric nanogenerators,[15] nanoresonators,[16] photonic crystals,[17] photodetectcors,[18] optical modulator waveguides,[19] light-emitting diodes,[20] field emitters,[21] gas sensors,[22,23] solar cells,[24] and

* To whom correspondence should be addressed. E-mail: mjzheng@sjtu.edu.cn.
[†] Lab of CMSOEP, Department of Physics.
[‡] School of Chemistry & Chemical Technology.

(1) Ng, H. T.; Li, J.; Smith, M. K.; Nguyen, P.; Cassell, A.; Han, J.; Meyyappan, M. *Science* **2003**, *300*, 1249.
(2) Park, S.; Lim, J.-H.; Chung, S.-W.; Mirkin, C. A. *Science* **2004**, *303*, 348.
(3) Ponzoni, A.; Comini, E.; Sberveglieri, G.; Zhou, J.; Deng, S. Z.; Xu, N. S.; Ding, Y.; Wang, Z. L. *Appl. Phys. Lett.* **2006**, *88*, 203101.
(4) Fan, Z.; Lu, J. G. *J. Nanosci. Nanotechnol.* **2005**, *5*, 1561.
(5) Pan, Z. W.; Dai, Z. R.; Wang, Z. L. *Science* **2001**, *291*, 1947.
(6) Zheng, M. J.; Zheng, L. D.; Li, G. H.; Shen, W. Z. *Chem. Phys. Lett.* **2002**, *363*, 123.
(7) Wu, J. J.; Liu, S. C.; Wu, C. T.; Chen, K. H.; Chen, L. C. *Appl. Phys. Lett.* **2002**, *81*, 1312.
(8) Kong, X. Y.; Ding, Y.; Yang, R. S.; Wang, Z. L. *Science* **2004**, *303*, 1348.
(9) Gao, P. X.; Wang, Z. L. *J. Phys. Chem. B* **2002**, *106*, 12653.
(10) Lao, J. Y.; Huang, J. Y.; Wang, D. Z.; Ren, Z. F. *Nano Lett.* **2003**, *3*, 235.
(11) Yan, H. Q.; He, R. R.; Johnson, J.; Law, M.; Saykally, R. J.; Yang, P. D. *J. Am. Chem. Soc.* **2003**, *125*, 4728.
(12) Wang, Z. L.; Kong, X. Y.; Zuo, J. M. *Phys. Rev. Lett.* **2003**, *91*, 185502.
(13) Xu, C. X.; Sun, X. W.; Dong, Z. L.; Yu, M. B. *J. Cryst. Growth* **2004**, *270*, 498.
(14) Huang, M. H.; Mao, S.; Feick, H.; Yan, H.; Wu, Y.; Kind, H.; Weber, E.; Russo, R.; Yang, P. *Science* **2001**, *292*, 1897.
(15) Wang, Z. L.; Song, J. H. *Science* **2006**, *312*, 242.
(16) Bai, X. D.; Wang, E. G.; Gao, P. X.; Wang, Z. L. *Nano Lett.* **2003**, *3*, 1147.
(17) Chen, Y.; Bagnall, D.; Yao, T. *Mater. Sci. Eng., B* **2000**, *75*, 190.
(18) Liang, S.; Sheng, H.; Liu, Y.; Huo, Z.; Lu, Y.; Shen, H. *J. Cryst. Growth* **2001**, *225*, 110.
(19) Lee, J. Y.; Choi, Y. S.; Kim, J. H.; Park, M. O.; Im, S. *Thin Solid Films* **2002**, *403*, 553.
(20) Saito, N.; Haneda, H.; Sekiguchi, T.; Ohashi, N.; Sakaguchi, L.; Koumoto, K. *Adv. Mater.* **2002**, *14*, 418.
(21) Li, Q. H.; Wang, Q.; Chen, Y. J.; Wang, T. H.; Jia, H. B.; Yu, D. P. *Appl. Phys. Lett.* **2004**, *85*, 636.
(22) Lin, Y.; Zhang, Z.; Tang, Z.; Yuan, F.; Li, J. *Adv. Mater. Opt. Electron.* **1999**, *9*, 205.
(23) Fan, Z.; Wang, D.; Chang, P.-C.; Tseng, W.-Y.; Lu, J. G. *Appl. Phys. Lett.* **2004**, *85*, 5923.
(24) Law, M.; Greene, L. E.; Johnson, J. C.; Saykally, R.; Yang, P. *Nat. Mater.* **2005**, *4*, 455.

10.1021/ic7021598 CCC: $40.75
Published on Web 03/05/2008

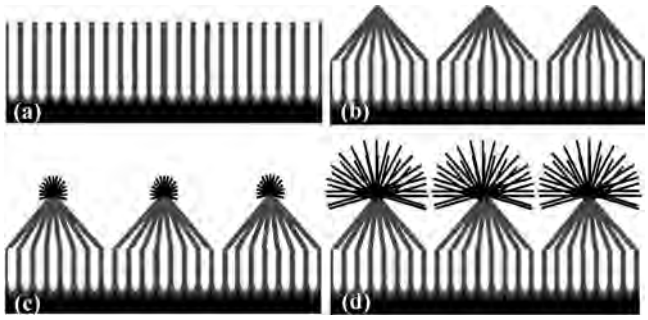

Figure 1. Schematic diagram of the process for the fabrication of lotus-leaf-like ZnO micro-nanostructures: (a) PAA films; (b) alumina nanowire pyramids; (c) various oriented ZnO nuclei formed on the top of alumina nanowire pyramids; (d) lotus-leaf-like ZnO micro-nanostructures on patterned PAA substrate.

so on. However, it still remains a big challenge to develop simple and reliable synthetic methods for hierarchical architectures with controlled morphology, orientation, and surface architectures, which strongly affect the properties of nanostructured materials. On the other hand, nearly all of the applications are based on its optical or electronic properties. In recent years, the superhydrophobic surfaces have received much attention due to their importance in fundamental research and promising applications.[25,26] Hong et al.[27] reported that the superhydrophobic surfaces with sufficiently high adhesive force had particular advantages to innovate design of open microfluidic devices for increasing needs of controlled transport of small liquids in biochemical separation, targeted drug delivery, immunoassay, etc. The superhydrophobic surfaces with high adhesive have been realized in aligned polystyrene nanotube films[28] and methyloctyldimethoxysilane self-assembled films.[29] Such sticking of droplets has been also reported for carbon nanotubes.[30] In this paper, we reported the fabrication of superhydrophobic lotus-leaf-like ZnO micro-nanostructure films with ultrastrong adhesive force by noncatalytic chemical vapor deposition (CVD), taking advantage of charged surfaces and morphologies of alumina nanowire pyramid substrates and ZnO properties (polar surfaces and oriented growth habits).

Figure 1 displays schematically the formation process of the lotus-leaf-like ZnO micro-nanostructures. The basic idea comes from the unique properties of both ZnO and porous anodic alumina (PAA) films. The variety of ZnO nanostructures benefits from the fact that ZnO has two polar surfaces and three fast growth directions.[8,14] On the other hand, it has been demonstrated that there are anion impurities (PO_4^{3-}, $C_2O_4^{2-}$, and OH^-) in the pore walls of PAA films,[31] and such localized negative charges play an important role in the growth of nanostructured ZnO materials.[32] When the PAA film (Figure 1a) was transformed into alumina nanowire pyramids (Figure 1b), the top of the pyramids where the alumina nanowires were more densely packed had higher negative charge density and hence a stronger electric field than other parts. Thus, it can be expected that ZnO nuclei should preferably form on the top of the pyramids (Figure 1c). In addition, the space between each pyramid allows ZnO nanorods to grow long in every possible direction. As a result, three-dimension (3D) gridlike ZnO microspheres made up of uniform ZnO nanorods were successfully realized on the top of the alumina nanowire pyramids due to the 3D interlaced growth of ZnO nanorods (Figure 1d). The method used to fabricate the lotus-leaf-like ZnO micro-nanostructure films is simple and of low cost because no metal catalyst is needed and the patterned alumina substrate can be easily obtained based on our previous work.[33]

2. Experimental Section

The PAA films were prepared through stable high-field anodization in a $H_3PO_4-H_2O-C_2H_5OH$ electrolyte system.[33] Round aluminum foil (99.999% purity, 0.25 mm thickness) with a diameter of 2 cm was used as the starting material. Before anodization, the aluminum foil was degreased in acetone, washed in deionlized water, and put into a tailor-made holder with a circular area of 2 cm^2 exposed to the electrolyte. The aluminum was electropolished at a constant voltage in a 1:4 volume mixture of perchloric acid and ethanol. Anodization was then carried out in a $H_3PO_4-H_2O-C_2H_5OH$ electrolyte system (concentration of H_3PO_4, 0.4 M) at 195 V and 3000 A m^{-2}. A large electrolytic cell (2 L), a powerful low-constant temperature bath, and a vigorous stirrer (800 rpm) were employed to keep the low temperature (−10 °C) required for the high-field anodization. Figure 2a shows a field-emission scanning electron microscopy (FESEM, Philips XL30FEG) image of PAA films formed by stable high-field anodization. The alumina nanowire pyramids were obtained by etching the PAA films in a mixed solution of 1.8% chromic acid and 6% phosphoric acid at 60 °C.

The lotus-leaf-like ZnO micronanostructures were synthesized in a horizontal tube furnace system by CVD. Pure zinc powder (99.99%) of 0.6 g was placed in an alumina boat located at the center of a horizontal quartz tube. The alumina nanowire pyramids were employed as the substrates and placed at the downstream position of the carrier gas, with the distance between Zn source and substrate being about 10 cm. The quartz tube was evacuated to about 2.0 Pa to remove the residual oxygen before heating. The source material was heated to 550 °C at a rate of 10 °C/min. Pure argon and oxygen were introduced at one end of the quartz tube at flow rates of 240 standard cubic centimeters per minute (sccm) and 60 sccm, respectively. The temperature was kept at 550 °C for 120 min; the work pressure was about 180 Pa. After being heated, the tube was cooled naturally to room temperature under the above-mentioned atmosphere, and white films were found covering the alumina substrates.

The hydrophobicity of the lotus-leaf-like ZnO micronanostructure films was measured by means of the water contact angle (CA) using

(25) Quere, D. *Rep. Prog. Phys.* **2005**, *68*, 2495.
(26) Feng, X. J.; Jiang, L. *Adv. Mater.* **2006**, *18*, 3063.
(27) Hong, X.; Gao, X. F.; Jiang, L. *J. Am. Chem. Soc.* **2007**, *129*, 1478.
(28) Jin, M. H.; Feng, X. J.; Feng, L.; Sun, T. L.; Zhai, J.; Li, T. J.; Jiang, L. *Adv. Mater.* **2005**, *17*, 1977.
(29) Song, X. Y.; Zhai, J.; Wang, Y. L.; Jiang, L. *J. Phys. Chem. B* **2005**, *109*, 4048.
(30) Wang, Z.; Koratkar, N.; Ci, L.; Ajayan, P. M. *Appl. Phys. Lett.* **2007**, *90*, 143117.
(31) Choi, J.; Luo, Y.; Wehrspohn, R. B.; Hillebrand, R.; Schilling, J.; Gösele, U. *J. Appl. Phys.* **2003**, *94*, 4757.
(32) Ding, G. Q.; Shen, W. Z.; Zheng, M. J.; Fan, D. H. *Appl. Phys. Lett.* **2006**, *88*, 103106.
(33) Li, Y. B.; Zheng, M. J.; Ma, L.; Shen, W. Z. *Nanotechnology* **2006**, *17*, 5101.

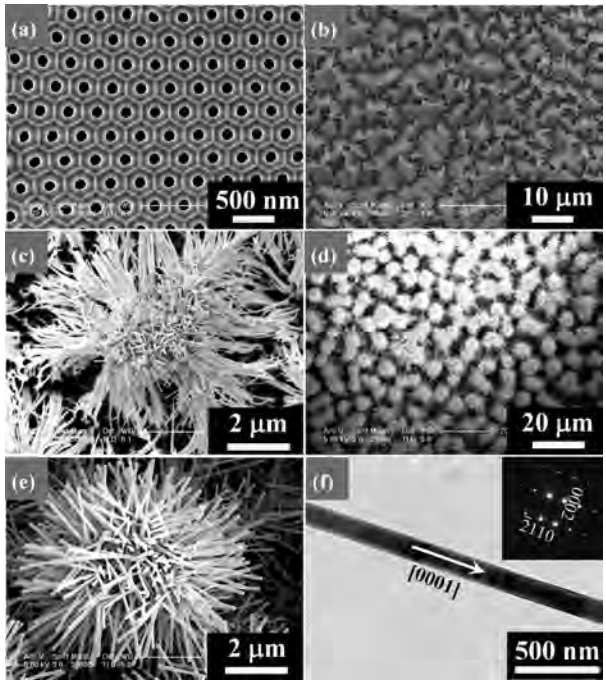

Figure 2. FESEM images of (a) PAA films, (b) alumina nanowire pyramids, (c) ZnO nuclei on the top of alumina nanowire pyramid, and (d) lotus-leaf-like ZnO micro-nanostructures, (e) magnified view of ZnO micro-nanostructures, and (f) TEM image of a single ZnO nanorod and corresponding electron diffraction pattern (inset).

an OCA 20 contact angle system (Data Physics Instrument GmbH, Germany) at ambient temperature.

3. Results and Discussion

As shown in Figure 2b, the size of each pyramid is about 4–6 μm. However, the hole-to-hole distance is about 350 nm, which shows that every pyramid is formed by many cells. Because the size of the resulting pyramids structure (4–6 μm) is the same as the size of ordered domain (Figure 2a) of the PAA films we use, we suppose the pyramid is formed by the cells within the same ordered domain. The self-ordering region (or ordered domain) of the PAA film means that within the region, the arrangement of the hexagonal cells is ordered. But between these regions (at the boundary), the arrangement of the cells is not ordered (Figure 2a only shows the cells within a self-ordering region). Because of the occurrence of defects or distortion in the pore walls at the boundaries between the ordered regions, the alumina cells dissolved faster at the boundaries than within the ordered regions. By choosing a proper etching time, cells at the boundaries were totally dissolved while those within the ordered regions were partially dissolved, forming alumina nanowires. These nanowires bent down and leaned against each other to form these alumina nanowire pyramids.

Figure 2d displays the FESEM image of the lotus-leaf-like ZnO micro-nanostructure films. The magnified FESEM image in Figure 2e reveals that every ZnO microsphere (similar to the micropapilla on lotus leaf surface) is assembled by over 200 various oriented ZnO nanorods (similar to the hairlike nanostructures on mircopapilla of the lotus leaf). The average size of these microspheres is about 7 μm, and their separation is about 10 μm. The diameter and length of individual ZnO nanorod were about 130 nm and 2–3 μm, respectively. The transmission electron microscope (TEM, JEOL JEM-2100F) and selected area electron diffraction (SAED) results in Figure 2f show that these ZnO nanorods are single crystalline and grow along the [0001] direction, which reveals good crystal quality of the nanorods.

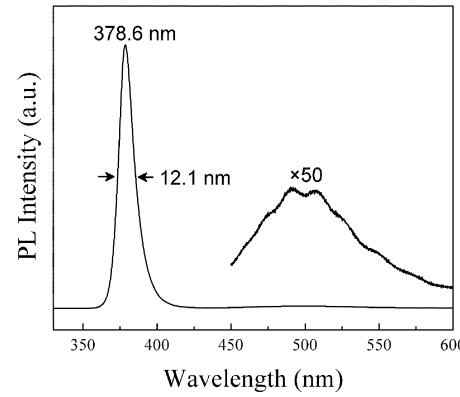

Figure 3. Room-temperature photoluminescence spectrum of the lotus-leaf-like ZnO architectures.

For confirming that the 3D gridlike microspheres grew on the top of the alumina nanowire pyramids, we observed the morphologies of the sample when the growth time was only 10 min. As shown in Figure 2c, dense and various oriented short ZnO nanorods can be observed only on the top of the alumina nanowire pyramid, which clearly demonstrates the above expectation. Above results indicate that the alumina nanowire pyramids play an important role in successfully realizing the fabrication of lotus-leaf-like ZnO micronanostructures films.

Figure 3 displays the room-temperature photoluminescence (PL) spectrum of the bushlike ZnO architectures. The room-temperature PL spectrum was measured by a Jobin Yvon ultraviolet–visible monochromator under a 325 nm He−Cd laser excitation. As shown in Figure 3, an intensive and sharp peak at 378.6 nm with the full width at half-maximum of 12.1 nm (∼105 meV) dominates the room-temperature PL spectrum of the bushlike ZnO architectures. For bulk ZnO, UV emissions were only observed at very low temperature, and the intensity of the emissions decreased rapidly with the increase of temperature due to the thermal quenching effect. Bagnall et al.[34] demonstrated that the improvement of the crystal quality (decrease of impurities and structure defects) could result in detectable UV emission at room temperature. Thus, the observation of intensive and sharp UV peak at room temperature in our experiment indicates that the ZnO nanorods have very little impurity and few structure defects. This can be confirmed by the fact that a very weak green emission band near 500 nm is observed in the PL spectrum, because the intensity of the green emission is determined by the concentration of the oxygen vacancies in the ZnO crystal.[35] Besides, the three-dimensionally interlaced structure of the bushlike ZnO architectures may also contribute to the

(34) Bagnall, D. M.; Chen, Y. F.; Shen, M. Y.; Zhu, Z.; Yao, T. *J. Cryst. Growth* **1998**, *185*, 605.
(35) Huang, M. H.; Wu, Y.; Feick, H.; Tran, N.; Weber, E.; Yang, P. *Adv. Mater.* **2001**, *13*, 113.

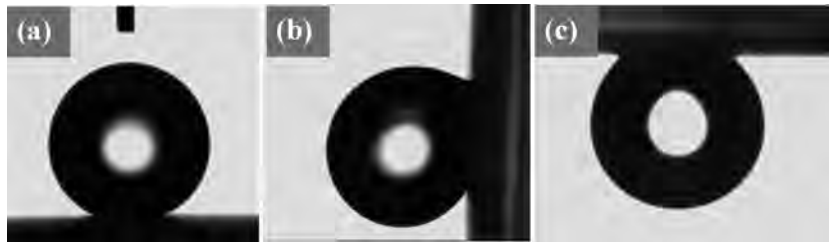

Figure 4. Shapes of the water droplets on the lotus-leaf-like ZnO micronanostructure films at tilt angles of (a) 0°, (b) 90°, and (c) 180°.

observation of intensive and sharp UV peak at room temperature. The appearance of intensive and sharp UV emission and very weak green emission in the PL spectrum further demonstrates that the bushlike ZnO architectures have good crystallinity.

Figure 4a shows the shape of a water droplet on the lotus-leaf-like ZnO micronanostructure films with water contact angle (CA) as high as 151°, which shows that the films have superhydrophobicity. The 3D spherical gridlike ZnO micronanostructures effectively increase the hydrophobicity compared with that of relatively flat ZnO films (CA = 109°).[36] It is also found that the water droplet does not slide when the film is tilted vertically (Figure 4b) or even reversed (Figure 4c). This phenomenon was also found in an aligned polystyrene nanotube film by Jin et al.,[28] of which the critical weight of the water droplet on a tilted nanotube layer at 90° is 8 mg. The critical weight of the water droplet on a reversed lotus-leaf-like ZnO micro-nanostructure film is as high as 20 mg, which indicates an ultrastrong adhesive effect between water and the film.

To explain these phenomena, Jin et al.[28] proposed that the high contact angle resulted from the large number of air pockets present due to the nanostructure of the composite surface, whereas the high adhesive force resulted from a large van der Waals force between the solid surfaces and water.[37,38] However, Li and Amirfazli challenged their explanations because they were not based on the same microscope mechanism.[39] Since the high nanotube density or fraction of nanotubes which is required for a high adhesive force will lead to a low contact angle according to Cassie−Baxter relation, they thought they even contradicted each other. Thus, it is necessary to explain the appearing contradiction based on the same microscope mechanism, and that is what we are trying to do in the following paragraph.

Generally, the apparent contact angle of a hydrophobic surface increases with its roughness, which is usually defined as the real surface area to the apparent surface area. However, it is actually the local roughness at the line of contact (also called the triple line) that determines the apparent contact angle. Thus, we can define the local roughness as the real length of the line of contact to the apparent length of the line of contact. The real length of the line of contact increases with the increase of surface roughness, which results in the increase of the apparent contact angle. For a surface with high roughness, due to the trapping of air pockets under the drop, the real length of the line of contact is largely increased, which results in a drastic increase in the apparent contact angle, as shown in the experiment of Johnson and Dettre.[40] The high contact angle for our sample is due to long real length of the line of contact achieved with the trapping of air pockets by the 3D interlaced structure. Meanwhile, the high adhesive force is also a result of the long real length of the line of contact. Considering that the surface is not flat but made of many nanorods, the van der Waals force is actually proportional to the real length of the line of contact, not to the area of the solid/liquid interface. Suppose when a rod is being pulled out of water, the van der Waals force that acts on the rod is actually at the line of contact. Besides, the capillary force acting on the line of contact will also contribute to the adhesive force, and apparently it is proportional to the real length of the line of contact. Therefore, both the high contact angle and high adhesive force resulted from the long real length of the line of contact.

4. Conclusion

In conclusion, the superhydrophobic lotus-leaf-like ZnO micronanostructure films with ultrastrong adhesive force were fabricated by the inducement of uniquely patterned PAA substrates. This provides a new approach to fabricating hierarchical architectures with special functional properties. The TEM results and PL spectrum of the hierarchical ZnO architectures indicate that they have very good crystallinity. It is expected that this superhydrophobic ZnO micronanostructure film with high adhesive force to liquid could be used in the future as a "mechanical hand" to transfer small liquid droplets for microsample analyses. Moreover, because of the favorable surface-to-volume ratio of the multidimensional ZnO nanostructures, they are expected to have potential applications in gas sensors, etc.

Acknowledgment. This work was supported by the Natural Science Foundation of China (Grant no. 50572064, 10734020), National Minister of Education Program IRT0524, and National Major Basic Research Project 2006CB921507.

IC7021598

(36) Sun, R-D.; Nakajima, A.; Fujishima, A.; Watanabe, T.; Hashimoto, K. *J. Phys. Chem. B* **2001**, *105*, 1984.
(37) Autumn, K.; Liang, Y. A.; Hsieh, S. T.; Zesch, W.; Chan, W. P.; Kenny, T. W.; Fearing, R.; Full, R. J. *Nature* **2000**, *405*, 681.
(38) Geim, A. K.; Dubonos, S. V.; Grigorieva, I. V.; Novoselov, K. S.; Zhukov, A. A.; Shapoval, S. Y. *Nat. Mater.* **2003**, *2*, 461.
(39) Li, W.; Amirfazli, A. *Adv. Mater.* **2007**, *19*, 3421.
(40) Johnson, R. E.; Dettre, R. H. *Adv. Chem. Ser.* **1964**, *No. 43*, 112.